remote sensing

MDPI

Article

Comparative Assessments of the Latest GPM Mission's Spatially Enhanced Satellite Rainfall Products over the Main Bolivian Watersheds

Frédéric Satgé [1,2,*], Alvaro Xavier [1], Ramiro Pillco Zolá [3], Yawar Hussain [4], Franck Timouk [5], Jérémie Garnier [1,2] and Marie-Paule Bonnet [2,6]

1 Instituto de Geociência (IG), Universidade de Brasília, 70910-900 Brasília-DF, Brasil; alvaroxavier.f@gmail.com (A.X.); garnier@unb.br (J.G.)
2 Mixed Laboratory International, Observatory for Environmental Change (LMI-OCE), IRD/UnB, Campus Darcy Ribeiro, 70910-900 Brasília-DF, Brasil; marie-paule.bonnet@ird.fr
3 Instituto de Hidráulica e Hidrología (IHH), Universidad Mayor de San Andrés, La Paz, Bolivia; rami_lund99@hotmail.com
4 Departamento de Engenharia Civil e Ambiental, Universidade de Brasilia, 70910-900 Brasília-DF, Brasil; yawar.pgn@gmail.com
5 Géosciences Environnement Toulouse (GET) (UMR 5563, IRD, CNRS), Université Paul Sabatier, 31062 Toulouse, France; franck.timouk@ird.fr
6 Espace Développement (ESPACE-DEV) (UMR 228, IRD), 34093 Montpellier, France
* Correspondence: frederic.satge@gmail.com

Academic Editors: Magaly Koch and Prasad S. Thenkabail
Received: 7 February 2017; Accepted: 9 April 2017; Published: 13 April 2017

Abstract: The new IMERG and GSMaP-v6 satellite rainfall estimation (SRE) products from the Global Precipitation Monitoring (GPM) mission have been available since January 2015. With a finer grid box of 0.1°, these products should provide more detailed information than their latest widely-adapted (relatively coarser spatial scale, 0.25°) counterpart. Integrated Multi-satellitE Retrievals for GPM (IMERG) and Global Satellite Mapping of Precipitation version 6 (GSMaP-v6) assessment is done by comparing their rainfall estimations with 247 rainfall gauges from 2014 to 2016 in Bolivia. The comparisons were done on annual, monthly and daily temporal scales over the three main national watersheds (Amazon, La Plata and TDPS), for both wet and dry seasons to assess the seasonal variability and according to different slope classes to assess the topographic influence on SREs. To observe the potential enhancement in rainfall estimates brought by these two recently released products, the widely-used TRMM Multi-satellite Precipitation Analysis (TMPA) product is also considered in the analysis. The performances of all the products increase during the wet season. Slightly less accurate than TMPA, IMERG can almost achieve its main objective, which is to ensure TMPA rainfall measurements, while enhancing the discretization of rainy and non-rainy days. It also provides the most accurate estimates among all products over the Altiplano arid region. GSMaP-v6 is the least accurate product over the region and tends to underestimate rainfall over the Amazon and La Plata regions. Over the Amazon and La Plata region, SRE potentiality is related to topographic features with the highest bias observed over high slope regions. Over the TDPS watershed, the high rainfall spatial variability with marked wet and arid regions is the main factor influencing SREs.

Keywords: IMERG; GSMaP; TMPA; Bolivia; assessment; GPM

1. Introduction

Accurate rainfall estimation is crucial to monitor long- and short-term hydro-climatologic variations. Drought and flood scenarios can be predicted or understood from the rainfall analysis,

protecting the local environment and increasing population security. In remote regions, few meteorological stations are available and are unevenly distributed due to difficulties of access for installation and maintenance. Over the last few decades, numerous Satellite Rainfall Estimates (SREs) were made available from different organizations allowing a high quality of rainfall monitoring over the same periods. Nowadays, a new generation of SREs is being made available to ensure continuity in rainfall monitoring, addressing previous SREs' deficiencies related to aging sensors. Two SRE groups, which are derived from the Global Precipitation Monitoring (GPM) mission launched on 27 February 2014, are now available. They are the Integrated Multi-satellitE Retrievals for GPM (IMERG) and the GPM Global Satellite Mapping of Precipitation (GSMaP-v6). Available at a 0.1° and half-hourly and hourly temporal scales, respectively, they offer the opportunity of capturing finer local rainfall variations in space and time. Data is available from March 2014 to present. However, IMERG and GSMaP-v6 products were released in early January 2015 and, thus, few studies have assessed their potentiality yet. A study compared IMERG, with TRMM Multisatellite Precipitation Analysis (TMPA) on a global scale at a monthly temporal step [1]. Differences between IMERG and TMPA estimates were related to surfaces type and precipitation rates with a tendency for IMERG to better capture major heavy precipitation regions. Over India, on a daily scale and using rain gauges as a reference, IMERG is more suitable to represent monsoon rainfall than GSMaP-v6 and TMPA gauges adjusted versions while GSMaP-v6 slightly outperformed IMERG and TMPA over low rainfall Indian regions [2]. Over Iran, in comparison with gauges measurements, IMERG daily estimates are more accurate than TMPA considering categorical and quantitative statistical analysis [3]. Over China, in comparison with rain gauge estimates, IMERG monthly estimates are more accurate than TMPA [4] with the same observations made at daily and sub-daily scales [5]. Due to the small number of publications about GPM-derived SREs, there is still a need for more assessment studies in other regions of the globe. This is even true when considering GSMaP-v6 as there is only one study reported on its accuracy assessment [2]. In this context, we assessed for the first time IMERG and GSMaP-v6 over Bolivia, using 247 rain gauges as a reference. Bolivia is a very interesting region for such studies, as it includes very wet, wet, and semi-arid to arid regions corresponding to the Amazon, La Plata and Altiplano watersheds, respectively. Therefore, the SREs can be assessed for both heavy and low rainfall amounts as well as intensity. These regions are separated by the Andean Cordillera resulting in high elevation variation ranging over the country from few hundred meters to more than 6000 m. Thus, variable rainfall processes are observable and the SREs ability can be evidenced in relation to dominant rainfall processes. Here, IMERG and GSMaP-v6 are assessed for the very first time in Bolivia at annual, monthly and daily scales over the three main hydrological watersheds (Altiplano, Amazon and La Plata) separately for both wet and dry seasons. Topography is a well-known factor influencing SREs and, generally, SREs are more biased over mountainous regions than over relative flat regions [6–8]. Therefore, a complementary analysis regarding the topographic influence is done by assessing SREs' potentiality over different slope classes for each national watershed separately. In previous studies [9,10], TMPA was found to provide the most accurate SREs over the country, in comparison to Climate prediction center MORPHing (CMORPH), Precipitation Estimation from remotely Sensed Information using Artificial Neural Networks (PERSIANN), GSMaP-v5, Climate Forecast System Reanalysis and Reforecast (CFSR) and Modern-Era Retrospective Analysis for Research and Application (MERRA) products considering annual, monthly and daily rainfall amount. Thus, TMPA is considered to observe the potential enhancement brought by IMERG and GSMaP-v6 products.

2. Materials and Methods

2.1. Study Area

Bolivia is located in central South America with an extent close to 1,100,000 km^2. Elevation ranges between 75 and 6549 m following an increasing east-west pattern from the Amazon to the Altiplano region. Bolivia can be divided into three main watersheds: The Titicaca, Poopó, Desaguadero and

Salar system (TDPS), La Plata and Amazon with a superficial extent of approximately 149,000, 226,000 and 716,000 km^2, respectively (Figure 1a). The Altiplano region is trapped between the occidental and oriental cordillera at a mean elevation of 4000 m with mean slope value of 4.7° [11,12]. The climate throughout the region is semi-arid with mean rainfall of 350 mm (1998–2015). According to SRTM and TMPA data [9,12], the Amazon region is located at a mean elevation of 680 m with a mean slope value of 5.3° and a mean annual rainfall of 1550 mm (1998–2015). Finally, the La Plata watershed presents a mean elevation of 1350 m for a mean slope value of 7° and a mean annual rainfall of 850 mm (1998–2015).

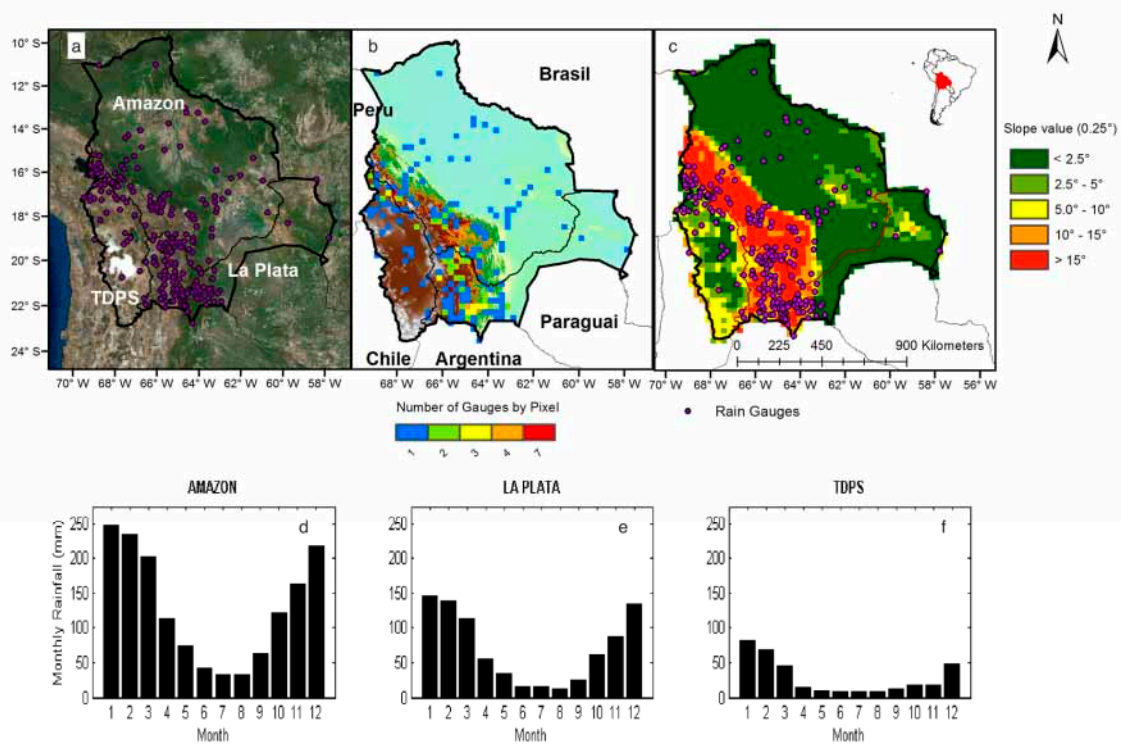

Figure 1. The study area (**a**) with the number of rain gauges included in studied 0.25° SREs pixels (**b**) 0.25° mean slope pixel derived from SRTM-GL1 (**c**) and mean monthly rainfall amounts derived from TMPA for the 1998–2015 period for each considered regions (**d**–**f**).

2.2. Datasets

IMERG is a product of the National Aeronautics and Space Administration (NASA). Rainfall estimate algorithms involve components from the previous algorithms of TMPA, CMORPH and PERSIANN rainfall estimates. IMERG uses both passive microwave (PMW) and infra-red (IR) sensors available from Low Earth Orbital (LEO) and geostationary satellites, respectively. Firstly, rainfall estimates are derived from PMWs using the Goddard profiling algorithm 2014 (GPROF2014) [13] and IR rainfall estimates provided by the Climate Prediction Center (CPC). Then, the CMORPH–Kalman filter Lagrangian time interpolation is used to produce half-hourly estimates from PMW and IR estimates. Finally, an adjustment of rainfall estimates is made by using the Global Precipitation Climatology Centre's (GPCC) figures for monthly precipitation. Three stage levels of IMERG rainfall estimates are available, and are called Early-, Late- and Final Run, respectively. The Early- and Late Run only use PMW and IR data while the Final Run includes a GPCC adjustment. All the products are delivered at half-hourly, daily and monthly scales on at 0.1° grid box. In this study, we used the IMERG Final Run (called IMERG hereafter).

GSMaP-v6 is a product of the Japan Science and Technology (JST) agency under the Core Research for Evolutional Science and Technology (CREST). GSMaP-v6 uses a combination of PMW and IR data

from CPC. The algorithms used to retrieve the rainfall rate from PMWs utilize brightness temperature. IR data from CPC merged at 4 km are used to increase the temporal and spatial resolutions. To do so, a Kalman filter refined PMW rainfall estimation propagation by using the atmospheric moving vector derived from two successive IR images [14]. In comparison to the previous GSMaP-v5, GSMaP-v6 includes new algorithms to enhance rainfall estimates over land and ocean [15]. GSMaP-v6 is available in the form of near-to-real-time and post-adjusted versions. In this study, we used the post-adjusted version of the GSMaP-v6 gauge, which is gauge-adjusted by using daily CPC global rain gauge data set.

TMPA is a product of NASA in collaboration with the Japan Aerospace Exploration Agency (JAXA). It provides rainfall estimates at a 0.25° spatial resolution over 50°N to 50°S at a 3-hourly temporal scale. Passive microwave (PMW) radiometers on board LEO satellites are used to estimate rainfall rates. IR data from the CPC of the National Weather Service/NOAA (CPC-IR here-after), from the Meteorological Operational satellite program (MetOp) and from the 0.07° Grisat-B1 are used to fill the gaps between PMW measurements [16]. There is a Real Time version (TMPA-RT v7) based only on PMW and IR data, and an adjusted version (TMPA-Adj v7) using gauge-based data from GPCC and Climate Assessment and Monitoring System (CAMS). In this study, we used the TMPA-Adj v7 (called TMPA hereafter).

The Servicio Nacional de Hidrología y Meteorología (SENAMHI) of Bolivia is in charge of the national hydro-meteorological network stations. For this study, SENAMHI provided the daily rainfall data of 247 stations over the regions for the 2014–2016 period. TDPS, La Plata and Amazon regions count with 37, 111 and 99 rain gauges, respectively (Figure 1a). The stations are distributed on 233 SRE 0.1° and 187 SRE 0.25° spatial resolution pixels.

2.3. Method Used

2.3.1. Pre-Process

For the inter-comparison with TMPA, GSMaP-v6 and IMERG were resampled to the 0.25° grid box [4]. To do so, GSMaP-v6 and IMERG were first sampled from 0.1° to 0.05°, then the rainfall at the 0.25° was obtained by taking the mean rainfall value of the 5 pixels (0.05°) included into the 0.25° pixel. At each rain gauge location, daily and monthly rainfall series were derived from the gauges and the corresponding TMPA, IMERG and GSMaP-v6 pixels. GSMaP-v6 and IMERG were cumulated from hourly and 30 min, respectively, to derive daily and monthly temporal series at 0.25° and 0.1° resolution. TMPA was cumulated from 3-hourly to derive daily and monthly temporal series at 0.25° resolution. When various gauges were available on a single pixel (Figure 1b), the mean rainfall value of all gauges included in the corresponding pixel was computed.

Finally, the digital elevation model SRTM-GL1 [12] was used to derive the mean slope value in the 0.25° grid box (Figure 1c). Slope values were computed at the native 1 arc second SRTM-GL1 mesh-size and resampled to the 0.25° grid box by meaning the slope value corresponding to each 0.25° grid box.

2.3.2. Comparison Methodology

First, annual rainfall maps were generated from IMERG and GSMaP-v6 at both 0.1° and 0.25° scales and from TMPA at 0.25° resolution to highlight the SREs' ability to represent regional patterns (Figure 2). For comparison, a rainfall map was derived from the 247 available gauges at the 0.25° using the Inverse Distance Weight (IDW) interpolation. Additionally, comparisons between gauges and SREs were done at the national scale and for each watershed separately, considering Coefficient Correlation (CC), Root Mean Square Error (RMSE) in percent and Bias in percent at both 0.1° and 0.25° grid box (Table 1).

Secondly, SREs were assessed at the monthly scale by comparing monthly SREs and gauge estimates. Comparisons between gauges and SREs were done at the national scale and for each watershed separately. At each considered spatial scale, CC, RMSE, Bias and Standard Deviation (STD)

were computed considering all months and for dry and wet seasons, separately, to observe the seasonal variability in the SREs' ability. Wet and dry seasons extend from November to March and from April to October, respectively (Figure 1d–f). For IMERG and GSMaP-v6, statistical scores were computed at both 0.1° and 0.25° scales to observe the potential enhancement introduced by the finer 0.1° resolution. To facilitate the interpretation of CC, RMSE and STD, the results are presented in form of Taylor diagram [17] (Figure 3). The Taylor diagrams allow a direct comparison between SREs by offering the opportunity to consider STD, CC and RMSE as a whole. RMSE and STD values were normalized to allow comparison between watersheds as rainfall amounts differ from one to another watershed (Figure 1d–f). The normalization process was made by dividing the SREs RMSE and STD values by the STD of the reference. As a result, in the Taylor diagrams, the reference is represented by the dot black point in which, the STD, RMSE and CC values are equal to 1, 0 and 1, respectively. Therefore, the lower the distance between the SREs and reference, the closer the SREs and reference rainfall estimates are. Additionally, Bias values are presented in Table 2 to observe the potential over/under estimation of each considered SRE. RMSE in percent and CC are also presented in Table 2 to complete the Taylor diagram analysis. To observe the topographic influence on monthly SREs from TMPA, IMERG and GSMaP-v6, a supplementary analysis was performed. For each national watershed (Amazon, La Plata and TDPS) the mean slope value at each 0.25° pixel derived from SRTM-GL1 (Figure 1c) was used to separate the 187 0.25° grid box pixels in 5 slope classes. The five considered slope classes are 0°–2.5°, 2.5°–5°, 5°–10°, 10°–15° and >15°. Each class gathered, respectively, 23, 5, 7, 22 and 26 pixels for the Amazon region, 8, 1, 12, 32 and 19 pixels for the La Plata region and 8, 10, 11, 2 and 0 pixels for the TDPS region. For each region and classes, CC, RMSE and Absolute Bias (AB) were computed considering all months (Figure 4 and Table 3). The seasonal assessment of this study shows high variation in Bias values oscillating between positive and negative value according to the considered season. Thus, to avoid seasonal effects on the interpretation of result, we preferred the use of the AB value instead of bias value. The assessment was not done at the national scale as topographic effects are expected to vary in function to the regional rainfall pattern. Therefore, topographic effects would be different from one region to another and difficult to observe at the national scale. The analysis was only performed at the 0.25° grid box size as close to similar accuracy in IMERG and GSMaP-v6 are observed for 0.1° and 0.25° grid box size.

Finally, a daily analysis using categorical statistical analysis was done considering both all days and wet and dry seasons, separately. Rainfall amounts were considered as discrete values with only two observable cases: rainy day or not. A rainy day is considered when the precipitation amount is greater than or equal to a prescribed threshold (mm day^{-1}). For pixels including more than one rain gauge, the mean daily rainfall from all rain gauges was considered. It is noteworthy that some authors consider a pixel to be rainy when any of the gauges observed a rainfall amount greater or equal to the prescribed threshold. This consideration allows the consideration of the rainfall variability at the pixel scale [6]. However, such consideration requires the availability of various gauges into the considered pixel. In this study, only a few pixels count for more than one rain gauge and are mainly located over the La Plata region. Therefore, to get a homogeneous assessment over the entire study area, we did not use such a methodology. Here, we fixed the threshold value to 1 mm day^{-1}, as used by [18]. Four cases are possible: both SRE and rain gauge report a rain event (a), only SRE reports a rain event (b), only rain gauge reports a rain event (c) or neither SRE nor rain gauge report a rain event (d).

According to this characterization, several statistical parameters can be computed: the Probability of Detection (POD), the False Alarm Ratio (FAR), the Critical Success Index (CSI) and the Bias (B) (Equations (1)–(4)) [9,18–23].

$$\mathrm{POD} = \frac{a}{(a+c)} \quad (1)$$

$$\mathrm{FAR} = \frac{b}{(a+b)} \quad (2)$$

$$CSI = \frac{a}{(a+b+c)} \tag{3}$$

$$B = \frac{(a+b)}{(a+c)} \tag{4}$$

POD is an indicator of the SRE's ability to correctly forecasts rain events. Values vary from 0 to 1, with 1 as a perfect score.

FAR is an indicator of how often SREs detect a rain event when, actually, it does not occur. Values vary from 0 to 1, with 0 as a perfect score. FAR is also represented in form of the Success Ratio (SR = 1 − FAR).

CSI is the ratio between the number of a rain events correctly detected by the SRE and the number of all rain events registered by the gauge and the SRE data. Values vary between 0 and 1 with a perfect score of 1.

B is the ratio of satellite rain estimates to actual precipitation events. A B value above or below 1.0 implicates that the SRE overestimates or underestimates the number of rain events in a considered period.

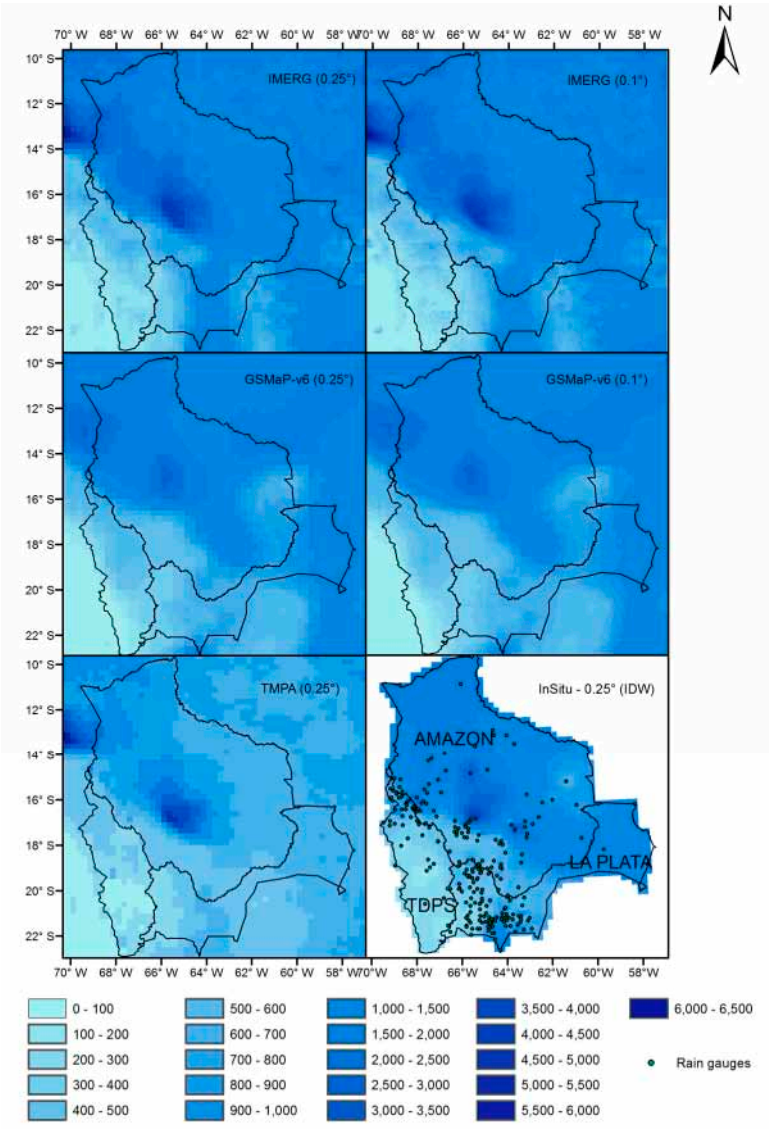

Figure 2. Annual rainfall pattern for all SREs. Rainfall amounts are in mm.

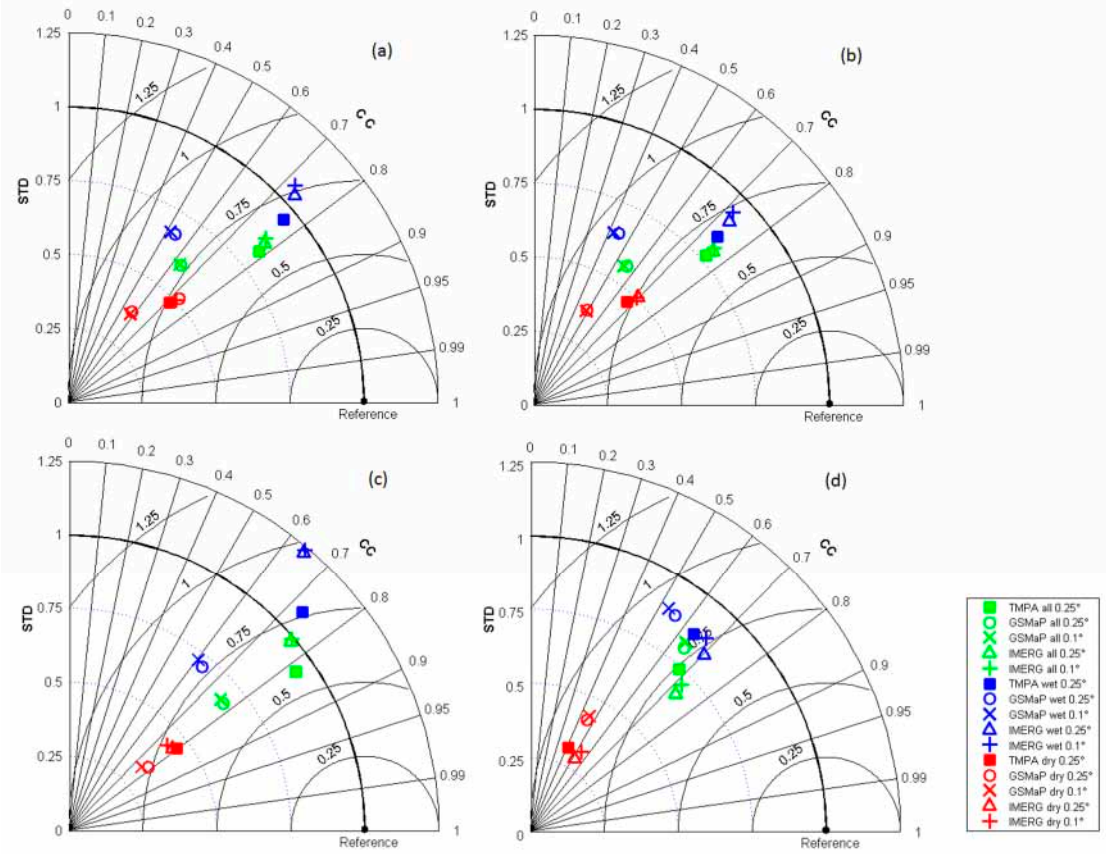

Figure 3. Taylor diagram for monthly rainfall considering the whole Bolivia (**a**), Amazon (**b**), La Plata (**c**) and TDPS (**d**) regions separately. The continuous curved lines represent RMSE values.

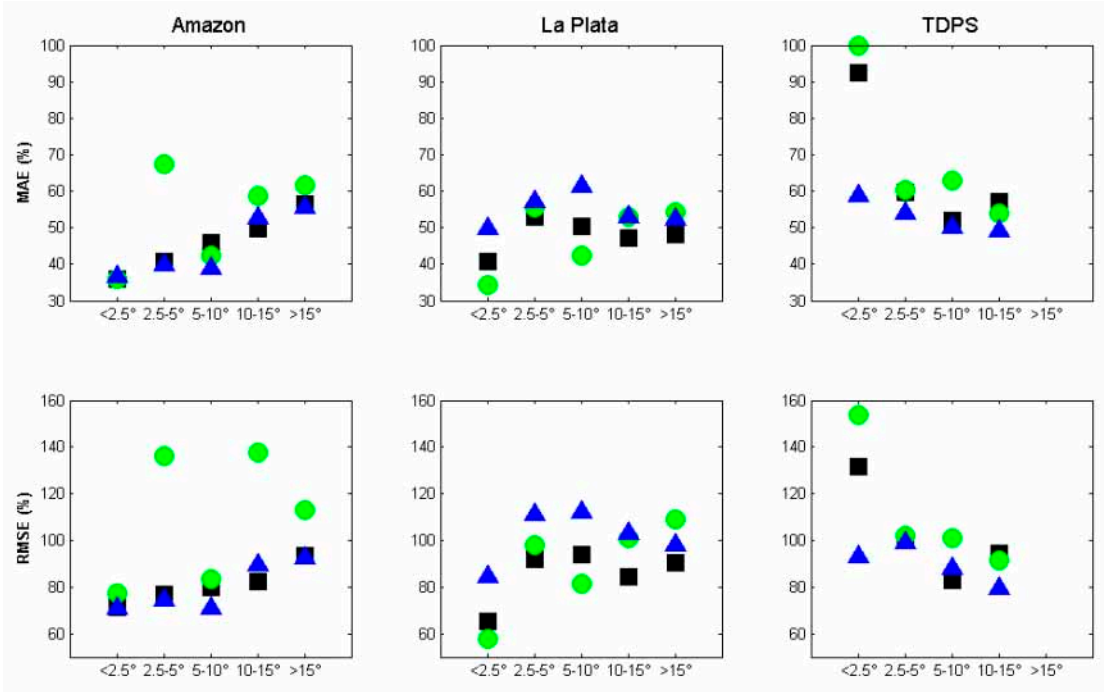

Figure 4. Absolute Bias (%) and RMSE (%) for different slope classes. Black squares, blue tringle and green point represent TMPA, IMERG and GSMaP-v6, respectively.

In the same way as for the monthly analysis, the results are presented in form of a synthesis diagram to consider POD, FAR, CSI and B as a whole in order to facilitate SREs' inter-comparison. The performance diagram [24] is used in this study as it was previously used for daily rainfall analysis over the Brazilian Amazon region [18]. The geometric relationship between SR, POD, B and the CSI is used to construct the performance diagram. Thus, the perfect forecast is lying in the upper right region of the diagram (Figure 5). Additionally, POD, FAR, CSI and B values are presented in Table 4 to complete the Performance diagram analysis. To complete the assessment, SREs' potentiality at the daily scale was also assessed, considering the mean slope classes used at the monthly scale. For each watershed, POD and FAR were computed for TMPA, IMERG and GSMaP-v6 for all considered classes (Figure 6). The topographic analysis was only performed at the 0.25° grid box size as close to similar accuracy in IMERG and GSMaP-v6 are observed for 0.1° and 0.25° grid box size.

3. Results and Discussion

3.1. Annual Scale

Figure 2 represents the annual rainfall maps for IMERG, GSMaP-v6 and TMPA for the 2014–2015 hydrological year. Over the region, with regard to annual maximum a great discrepancy is observed between SREs. A maximum value close to 3000, 5000 and 6400 mm year^{-1} is observed for GSMaP-v6, TMPA and IMERG. These high annual rainfall amount values are related to the especially strong ENSO anomaly which occurred that year, causing historical flooding in the Amazon watershed [25]. TMPA and IMERG seem more sensitive to extreme rainfall than GSMaP-v6 with higher rainfall amount observed which are closer to the maximum observed from gauge measurements (Figure 2). Similar CC, RMSE and Bias value from both IMERG and TMPA were obtained while GSMaP-v6 considerably underestimated rainfall amount by 30% (Table 1).

In the Amazon region, the two previously-evidenced rainfall hotspots [26] in the north-west corner and central amazon region are well detected by all SREs. In a general sense, GSMaP-v6 rainfall pattern is smoother than IMERG and TMPA. For example, over the TDPS, GSMaP-v6 has better captured the typical north-south decreasing rainfall patterns. However, the rainfall amount was poorly retrieved from GSMaP-v6 with the lowest CC and highest Bias and RMSE value among considered SREs and for all considered regions (Table 1).

TMPA and IMERG rainfall patterns are very close as they include very similar sensors and algorithm to retrieve rainfall. It is noteworthy that TMPA presents some spurious pixels with anomalous rainfall amounts relative to their neighboring pixels. This is clearly observable over the TDPS southern western parts. These pixels were well removed from IMERG estimates. This feature was already observed in China [4]. Here and in China, this occurs over regions with low rainfall amounts, showing TMPA difficulty over arid regions and the enhancements brought by the new IMERG over TMPA. In the actual context of climate variability and increased water usage for agriculture purpose over the TDPS region [27], IMERG offers great potential for regional monitoring and protection.

Indeed, IMERG presents a slightly better statistical score than TMPA over the TDPS region (Table 1). The finer 0.1° grid box size did not provide more accurate SREs, with similar statistical scores being observed for IMERG and GSMaP-v6 for all considered regions.

Table 1. Annual Bias (%), RMSE (%) and CC for TMPA, IMERG and GSMaP-v6.

	TMPA			**IMERG**						**GSMaP-v6**					
	Bias	**RMSE**	**CC**	**Bias**		**RMSE**		**CC**		**Bias**		**RMSE**		**CC**	
	0.25°	**0.25°**	**0.25°**	**0.1°**	**0.25°**	**0.1°**	**0.25°**	**0.1°**	**0.25°**	**0.1°**	**0.25°**	**0.1°**	**0.25°**	**0.1°**	**0.25°**
Bolivia	3.6	55.4	0.8	4.1	3.4	55.6	55.9	0.79	0.79	−25.1	−25.1	81.1	81.2	0.52	0.53
Amazon	1.8	53.4	0.76	3.1	3.5	52.8	52.3	0.78	0.77	−31.5	−30.7	83.5	81.3	0.38	0.38
La Plata	6.2	45.1	0.7	8.3	5.7	51.6	52.8	0.6	0.59	−19.7	−19.4	53.8	54.5	0.6	0.6
TDPS	7.9	54	0.63	−6.1	−5.6	49	51.5	0.68	0.67	−4.1	−2.8	55.9	56.8	0.53	0.54

3.2. Monthly Scale

Figure 3 presents the Taylor diagram for monthly rainfall for all the considered regions. Generally, all SREs performed better during the wet season than during the dry season. During dry seasons, rainfall amounts are lower and shorter in time, making their detection complicated by PMWs sensors [28,29]. During wet seasons for all considered regions, TMPA presents CC higher than 0.7, RMSE close to 50% and Bias values into the −10%–10% intervals (Table 2; Figure 3). These specific values were previously defined as objective values to ensure the good performance of SREs at monthly scale [9,10,19,30]. Results over the TDPS and for TMPA are in line with a previous study of the 2005–2007 period [9] with similar CC, RMSE and Bias values. Thus, the change in calibration procedure due to the end of TRMM Precipitation Radar estimates in October 2014 did not have a significant impact on TMPA rainfall estimates over Bolivia.

Regarding IMERG, at the 0.25° mesh size and global scale, statistical results are very close to TMPA and thus IMERG keeps on measuring rainfall at the same accuracy level as TMPA (Figure 3, Table 2). However, during the wet season, TMPA is slightly more suitable than IMERG due to its closer relative position to the dot-pointed reference (Figure 3); and IMERG is slightly more accurate than TMPA during the dry season, with lower Bias and RMSE and higher CC (Figure 3 and Table 2).

Some discrepancies are observed along the considered regions. Over the Amazon region, IMERG and TMPA performances are very similar (Figure 3), with close Bias, CC and RMSE values (Table 2). As for the global scale (Bolivia), TMPA slightly outperforms IMERG during the wet season and the opposite case is observed during the dry season (Figure 3, Table 2). Over the TDPS region, IMERG outperforms TMPA for all the considered seasons (Figure 3). This confirms the annual observation, with some pixels anomalously biased in relation to their neighboring pixels in both this study and that conducted over a similar region in China [4]. However, IMERG still slightly underestimates monthly rainfall amounts, as a negative bias of −18.2% is observed (Table 2). A higher discrepancy between IMERG and TMPA is observed over the La Plata river watershed. In this region, TMPA highly outperforms IMERG during the wet season with lower RMSE and higher CC (Figure 3; Table 2). Over this region, reference rainfall amounts are lower than in the Amazon (Figure 1d,e), and gauges are located over high, rough relief regions (Figure 1c). Indeed, the mean regional slope is estimated at 7°, according to SRTM-GL1 measurements, which have remained higher than the values of 4.7° and 5.3° registered for the TDPS and Amazon region, respectively. Thus, IMERG estimates are more affected by local relief and rainfall intensities than TMPA. These differences are characterized by lower CC and a RMSE increase of 18%. The future improvements brought to IMERG algorithms should focus on those specific features (rainfall amount and relief), to at least continue measuring rainfall estimates with the same accuracy trend as TMPA.

Passing from 0.1° to 0.25° grid box did not have a significant influence on rainfall estimate accuracy with quite similar CC, RMSE and Bias values at both 0.1° and 0.25° grid box for all regions and seasons (Figure 3; Table 2). For comparison, the spatial aggregation of SREs grid box was already found to be insignificant over the Altiplano (TDPS) considering TMPA estimates [21].

GSMaP-v6 is the least accurate considered SREs over the whole Bolivia with very high RMSE value higher to 100%, Bias values lower to −20% and low CC value lower to 0.7 (Table 2; Figure 3). None of the considered parameters fit the previously defined quality thresholds. The lower annual rainfall estimates observed for GSMaP-v6 in comparison to TMPA, IMERG and rain gauges (Figure 2) is confirmed by negative bias value at both 0.1° and 0.25° scales. GSMaP-v6 underestimates monthly rainfall at global scale and over the Amazon and La Plata regions at seasonal scale and for both dry and wet periods. GSMaP-v6 bias is lower over arid TDPS region with positive bias value. This shows the slight enhancement of GSMaP-v6 estimate over the TDPS arid region, and is in line with results observed over low-rainfall regions in India [2].

As observed for IMERG, the resampling step from 0.1° to 0.25° mesh size did not affect GSMaP-v6 estimates with very close relative position of both GSMaP-v6 at 0.25° and 0.1° in the Taylor diagrams (Figure 3) and close statistical score (Table 2).

Regarding the topographic assessment, very different patterns are observed from one region to another. Over the Amazon region, and for all SREs, the AB and RMSE values tend to increase with slope value while the opposite is observed over the TDPS region with a decrease of AB and RMSE values when mean slope value increase. Topography is known to affect SREs, and so do the rainfall amounts. Indeed, higher biases are generally observed over mountainous regions, and SREs are less accurate over arid regions in comparison to wet regions [6,8,9]. As a humid region, the Amazon region is well suited to observing topographic effects, because SREs' accuracy is not affected by low rainfall amounts (arid regions). Thus, the only factor altering SREs' accuracy in space is the topography. Actually, from lowlands to mountainous regions, AB and RMSE increased by approximately 20% for both IMERG and TMPA, and by approximately 30% for GSMaP-v6 (Figure 4 and Table 3). Over the TDPS region, the rainfall pattern follows a marked north-south gradient with rainfall amount decreasing from north to south. This typical rainfall pattern controls SREs' potentiality with SREs being more accurate in the northern, humid part than over the southern, more arid, part [9]. In this study, pixels with higher slope values are located in the northern part (high rainfall amount) while pixels with low slope value are located in the southern part (low rainfall amount) (Figure 1c). As a result, AB and RMSE values decreased by close to 10%, 20% and 50% for IMERG, TMPA and GSMaP-v6 from low to high slope region (Figure 4 and Table 3). Therefore, over the TDPS region the climatological context is the predominant factor influencing SREs' accuracy in space, rather than topographic effects. It is noteworthy that for all considered slope classes, IMERG presents close to the lowest AB and RMSE values, and higher CC values, confirming the higher performance previously observed over the same region for the annual and monthly seasonal comparisons (Figure 3, Tables 1 and 2). Over the La Plata region, no 'linear' relation is observed between topographic effect (slope value) and the SREs' accuracy. However, topographic influence is still observed with lower AB and RMSE values over the flat regions (slope <2.5°). Between the first class (<2.5°) and second class (2.5°–5°), all SREs present a positive gap in AB and RMSE values remaining high and relatively constant for all next classes (Figure 4 and Table 3). The observed AB increase between flat region class (slope <2.5°) and the rest of the considered classes is of approximately 10% for both IMERG and TMPA and close to 20% for GSMaP-v6. This non-linear trend between SRE accuracy and slope value should be related to the rain gauges' distribution. Indeed, most of the gauges with slope values higher than 2.5° are located and trapped in high-slope regions (Figure 1c). As a result, for those pixels there is a high discrepancy between neighboring slope values, which is not observed for the pixels with slope value lower than 2.5° (Figure 1c). Therefore, pixels with slope values above 2.5° are under a homogeneous topographic effect, expected to be similar among all classes that could explain the tendency observed in Figure 4.

In a general sense, IMERG keeps providing rainfall estimates as accurate as TMPA over the Amazon region, while offering the possibility to observe more local scale variation thanks to its lower grid box size. The main enhancement is observed over the TDPS arid region, where a slight increase in rainfall estimates is obtained from IMERG. However, over the mountain-dominated region of the La Plata head watershed, TMPA provides more accurate rainfall estimates than the new IMERG. The results evidence a relation between SRE accuracy and both seasonal and topographic contexts. SREs are generally more accurate during the wet season as rainfall amounts are higher than during the dry season. In the same way, SREs are more accurate over the low slope region as topographic effects are less important. In this context, it is noteworthy that the gauges' distribution influenced the observed results and conclusion. SREs' lower suitability observed over the La Plata region is partially explained by the distribution of the gauges. Actually, most of the gauges are located over the mountainous region where high slope values influence SREs (Figure 4). Different conclusions would have been dressed if the gauges were located over the low lands where slopes are lower and SREs would appear more efficient. In a similar way, over the TDPS region, most of the gauges are located on the northern wet part where SREs are known to be more accurate than over the southern arid region [9]. Different conclusions would have been achieved if the gauges were located on the southern

arid region. The potential intercomparison of SREs between the Amazon, La Plata and TDPS should be made with caution as different conclusions should be make from different rain gauge distribution.

Table 2. Monthly Bias (%), RMSE (%), and CC for TMPA, IMERG and GSMaP-v6 for both wet and dry seasons.

		TMPA 3B43			IMERG-FR (0.1°–0.25°)						GSMaP-v6 (0.1°–0.25°)					
		Bias	CC	RMSE	Bias (%)		CC		RMSE		Bias		CC		RMSE	
		0.25°	0.25°	0.25°	0.1°	0.25°	0.1°	0.25°	0.1°	0.25°	0.1°	0.25°	0.1°	0.25°	0.1°	0.25°
Bolivia	All	1.2	0.78	90.7	−2.3	−1.4	0.77	0.78	95.2	92.7	−22.6	−22.4	0.63	0.63	116.8	115.1
	Wet	5.7	0.76	64.2	−0.1	0.7	0.72	0.74	70.4	68.2	−20.9	−20.7	0.51	0.54	87	85.7
	Dry	−7.2	0.71	135.9	−6.5	−5.3	0.73	0.73	134.6	131.5	−25.9	−25.6	0.57	0.57	162.9	160.1
Amazon	All	0.5	0.75	82.7	−1.2	0.8	0.76	0.76	84.6	82	−30.1	−29.1	0.54	0.56	112	108.7
	Wet	6.2	0.74	59.7	1.9	3.3	0.72	0.73	63.5	60.7	−28.9	−28	0.42	0.44	87.9	84.5
	Dry	−8.5	0.67	117	−6.2	−3.2	0.69	0.7	114.7	112.8	−32	−30.7	0.49	0.49	142.4	140.1
La Plata	All	1.4	0.82	86.1	−10	−1.4	0.76	0.76	102.1	100.8	−17	−16.5	0.76	0.77	98.8	96.1
	Wet	4.9	0.73	63.3	−17	0.7	0.64	0.65	76	76.5	−16.4	−15.4	0.6	0.63	72.3	71.4
	Dry	−8.5	0.8	120.5	10.2	−7.2	0.76	0.79	132.8	122.6	−18.8	−19.7	0.75	0.78	135.6	129.2
TDPS	All	6.1	0.68	105.4	−17.4	−18.2	0.72	0.73	74.1	80.6	9.4	10.2	0.64	0.64	142.8	145.4
	Wet	4.9	0.64	58.6	−16.2	−16.8	0.67	0.7	41.6	44.8	11.2	11.6	0.53	0.56	80.2	80.8
	Dry	8.9	0.41	207.3	−20	−21.2	0.54	0.52	143.2	158.6	5.4	7.3	0.46	0.45	275.8	286.1

Table 3. Monthly AB (%), RMSE (%) and CC for TMPA, IMERG and GSMaP-v6 for different slope classes.

	Classes	TMPA			IMERG			GSMaP-v6		
		AB	RMSE	CC	AB	RMSE	CC	AB	RMSE	CC
Amazon	0°–2.5°	35.9	71.4	0.71	36.7	70.7	0.71	35.8	77.5	0.66
	2.5°–5°	40.8	76.8	0.80	39.9	74.1	0.81	67.3	136.3	0.16
	5°–10°	45.8	80.0	0.87	38.7	70.8	0.90	42.3	83.5	0.86
	10°–15°	49.8	82.2	0.85	52.8	89.5	0.82	58.7	137.7	0.41
	>15°	56.6	93.6	0.64	55.6	92.2	0.66	61.5	113.1	0.47
La Plata	0°–2.5°	40.8	65.3	0.87	49.6	84.6	0.75	34.4	57.9	0.86
	2.5°–5°	53.0	91.9	0.89	57.2	111.0	0.89	55.6	97.9	0.86
	5°–10°	50.5	94.0	0.81	61.3	111.8	0.79	42.3	81.5	0.83
	10°–15°	47.2	84.3	0.85	52.8	102.8	0.79	52.9	101.0	0.77
	>15°	48.0	90.6	0.79	52.3	97.8	0.75	54.2	108.8	0.71
TDPS	0°–2.5°	92.6	131.8	0.71	58.8	93.2	0.83	100.0	153.9	0.69
	2.5°–5°	59.8	99.8	0.56	53.8	99.0	0.61	60.4	101.9	0.56
	5°–10°	52.0	83.1	0.81	50.2	87.8	0.77	63.0	100.8	0.72
	10°–15°	57.1	94.5	0.84	49.0	79.5	0.90	53.9	91.2	0.79

3.3. Daily Scale

Figure 5 presents the POD, SR, CSI and B values for all SREs and all the considered regions in the form of a performance diagram. At the national scale and for all regions, all SREs better detect rainfall events during the wet season than during the dry season. As observed at the monthly scale, in the Amazon region, the ability of IMERG and TMPA to forecast daily rainfall are very similar (Figure 5). In the TDPS region, IMERG outperforms TMPA at both wet and dry season as its relative position to zero in Figure 5 is further than the relative TMPA position. This confirms the slightly better estimation observed at the monthly scale for IMERG in comparison to TMPA over the same region. With regard to the La Plata region, the ability of IMERG to detect daily rainfall is better than that of TMPA. However, TMPA remains more accurate at the monthly scale. Therefore, the relatively poor accuracy for monthly estimates observed for IMERG in comparison to TMPA over the same region seems to be linked to inaccuracy in daily rainfall amount estimates, rather than to their detection. Indeed, IMERG seems to underestimate daily rainfall amount as a negative monthly bias is observed (Table 2).

As noted for the monthly scale, the aggregation process from 0.1° to 0.25° does not change the ability of IMERG, according to the daily analysis. Indeed, both the 0.1° and 0.25° versions are very

close into the performance diagram for the Amazon and TDPS regions (Figure 5). Interestingly, over the La Plata region, the 0.1° grid box version of IMERG is slightly less suitable for discretizing rainy and non-rainy days. This confirms the general deficiency of IMERG at capturing the spatial variability of local rainfall induced by topographic features in this specific region. Passing from a 0.1° to a 0.25° grid box smoothed the rainfall spatial variability and should explain the slightly better ability of the 0.25° grid box version at the daily scale.

Regarding the topographic assessment, over the Amazon and La Plata regions, SREs' ability in differentiating rainy from non-rainy days decreases with the increase of slope value. For the Amazon region, POD and FAR respectively decrease and increase from flat- to high-slope regions. For the La Plata region POD decreases while the FAR remains relatively constant along the considered classes. Therefore, those observations agreed with monthly topographic assessment (Figure 6). Over the TDPS region, FAR decreased from flat- to high-slope regions, while no clear tendency is observed for the POD value along the considered classes. These results agreed with the monthly analyses, with the rainfall pattern as the main factor controlling SRE potential.

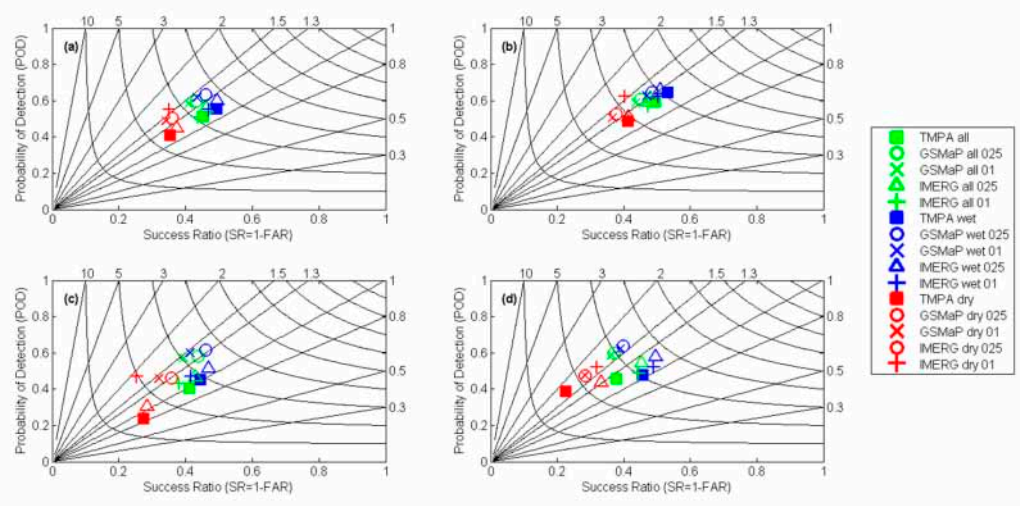

Figure 5. Performance diagram for the whole Bolivia (**a**), Amazon (**b**), La Plata (**c**) and TDPS (**d**) regions. Straight and curved lines represent the B and CSI values, respectively.

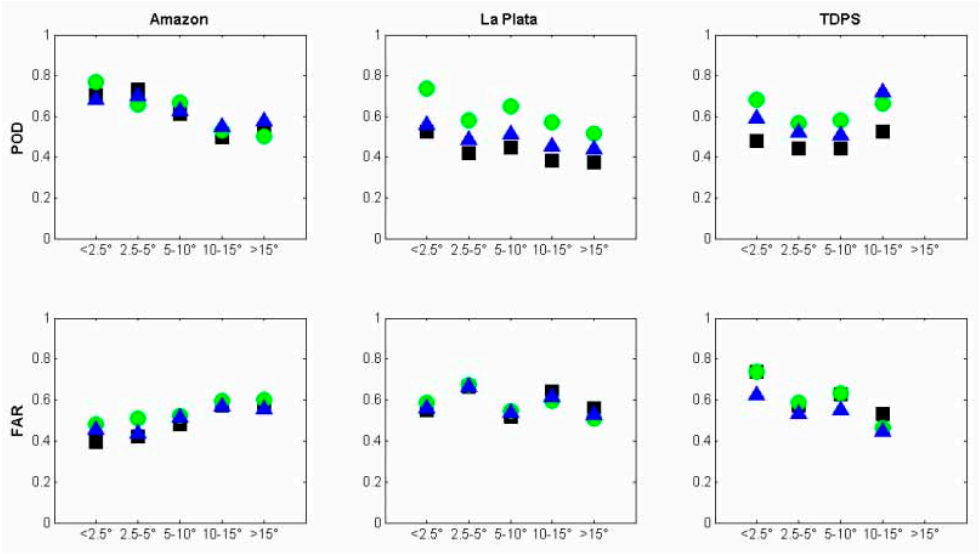

Figure 6. POD and FAR for different slope classes. Black squares, blue tringle and green point represent TMPA, IMERG and GSMaP-v6, respectively.

Table 4. POD, FAR, BIAS and CSI for TMPA, IMERG and GSMaP-v6 for both wet and dry season.

		TMPA				**IMERG**								**GSMaP-v6**							
		POD	**FAR**	**BIAS**	**CSI**	**POD**		**FAR**		**BIAS**		**CSI**		**POD**		**FAR**		**BIAS**		**CSI**	
		0.25°	**0.25°**	**0.25°**	**0.25°**	**0.1°**	**0.25°**	**0.1°**	**0.25°**	**0.1°**	**0.25°**	**0.1°**	**0.25°**	**0.1°**	**0.25°**	**0.1°**	**0.25°**	**0.1°**	**0.25°**	**0.1°**	**0.25°**
Bolivia	All	0.51	0.55	1.13	0.32	0.51	0.56	0.56	0.54	1.16	1.2	0.31	0.34	0.58	0.6	0.59	0.57	1.42	1.38	0.32	0.34
	Wet	0.55	0.51	1.12	0.35	0.55	0.6	0.53	0.5	1.17	1.2	0.34	0.37	0.62	0.63	0.57	0.54	1.42	1.37	0.34	0.36
	Dry	0.41	0.65	1.16	0.23	0.4	0.45	0.65	0.63	1.14	1.2	0.23	0.26	0.49	0.5	0.66	0.64	1.43	1.4	0.25	0.27
Amazon	All	0.59	0.51	1.2	0.37	0.57	0.61	0.53	0.55	1.21	1.27	0.35	0.37	0.59	0.61	0.56	0.52	1.35	1.35	0.33	0.35
	Wet	0.65	0.47	1.22	0.41	0.62	0.66	0.5	0.52	1.24	1.29	0.39	0.4	0.63	0.65	0.53	0.49	1.34	1.33	0.37	0.38
	Dry	0.49	0.59	1.18	0.29	0.46	0.51	0.6	0.62	1.13	1.23	0.27	0.3	0.51	0.53	0.63	0.59	1.38	1.39	0.27	0.28
La Plata	All	0.4	0.59	0.99	0.26	0.43	0.47	0.62	0.57	1.13	1.09	0.25	0.33	0.57	0.58	0.61	0.56	1.45	1.33	0.3	0.29
	Wet	0.45	0.56	1.02	0.29	0.47	0.51	0.58	0.53	1.13	1.09	0.28	0.36	0.6	0.62	0.59	0.54	1.45	1.34	0.32	0.32
	Dry	0.24	0.73	0.87	0.14	0.28	0.3	0.75	0.72	1.12	1.07	0.15	0.25	0.46	0.46	0.68	0.64	1.43	1.29	0.23	0.17
TDPS	All	0.46	0.62	1.21	0.26	0.49	0.54	0.55	0.55	1.1	1.61	0.3	0.33	0.59	0.6	0.64	0.63	1.62	1.2	0.29	0.3
	Wet	0.48	0.54	1.05	0.3	0.52	0.58	0.51	0.5	1.07	1.6	0.34	0.36	0.62	0.64	0.61	0.6	1.6	1.16	0.32	0.32
	Dry	0.39	0.78	1.72	0.17	0.38	0.44	0.68	0.67	1.2	1.66	0.21	0.23	0.48	0.47	0.72	0.72	1.68	1.31	0.22	0.22

4. Conclusions

The new GPM rainfall products were assessed for the first time in Bolivia at the annual, monthly and daily scales. The analysis was done at the national scale and for the three main watersheds (Amazon, La Plata and TDPS), separately, at both wet and dry seasons and for different slope classes. Generally, IMERG achieved its main objective of continuing to measure rainfall with the same accuracy as its predecessor, TMPA. However, some discrepancies are observed when considering different rainfall features over the regions. Over the wet Amazon region, at the annual and monthly scale, in comparison to gauge estimates, IMERG performs similarly to TMPA while TMPA is slightly more accurate than IMERG over the La Plata watersheds. This should be linked to the mountainous context that interferes on IMERG measurements quantification as IMERG was found to better discretize rainfall events occurrence. Over the TDPS arid region, IMERG better quantifies monthly rainfall in both wet and dry seasons. The enhancement of rainfall estimates over arid regions is very valuable for future hydro-climatic studies, as little changes in rainfall patterns have a strong impact on local water budgets. An interesting observed enhancement brought by IMERG in comparison to TMPA is its better ability to discretize rainy and non-rainy days for all considered regions and seasons. Therefore, it brings good perspective for future studies using the ratio of rainy to non-rainy days as a constraining factor in agriculture and drought monitoring. GSMaP-v6 is the least accurate SRE in Bolivia and for all considered regions and seasons. It underestimates monthly rainfall amounts over the Amazon and La Plata regions and overestimates rainfall over the arid TDPS region.

The study also showed a clear topography influence on the SREs' potentiality. SREs are most biased over mountainous region in relation to high slope values. This is clearly evidenced over the Amazon and La Plata region. However, such observation is not possible over the TDPS watershed, due to the rain gauges' distribution in relation to slope variability and the typical regional rainfall pattern. Over the TDPS, the rainfall pattern represents the main factor controlling SREs' potentiality. Along these lines, the study shows the importance of gauges' distribution in the assessment and the conclusions made, especially regarding the SREs' potential to compare different geomorphological climatic regions (Amazon, La Plata and TDPS). Indeed, different results and conclusions should be obtained from a different rain gauges' distribution giving more or less weight to slope and rainfall effects on SREs. Therefore, future study should base on a gauge network distribution, defined to represent topographic and rainfall patterns as well as possible.

In a general sense, the main advantage of IMERG and GSMaP-v6 is the higher spatial resolution of 0.1° that offers the opportunity to observe small local rainfall pattern variations. Therefore, GPM rainfall estimates open the opportunity to transfer SRE-based study from hydrological, drought, agriculture monitoring, initially used on a regional scale, to more local, unmonitored scales. Even if these two new SREs took advantage of a larger PMWs and IR sensors for their respective rainfall estimates, they do not always provide the most accurate estimates. Thus, we hope this timely study will be proven helpful in the near future for the enhancement of current algorithms used in IMERG and GSMaP-v6. Finally, the SREs' dependency on topographic effects should be used as guidelines for future SRE-related study over the region, in order to try and minimize topographic effects on SREs.

Acknowledgments: This work was supported by the Centre National d'Etudes Spatiales (CNES) in the framework of the HASM project (Hydrology of Altiplano: from Spatial to Modeling). The first author is grateful to the IRD (Institut de Recherche pour le Développement) and CAPES (Coordenação de Aperfeiçoamento de Pessoal de Nível Superior) Brazil for the financial support and to the SENAMHI-Bolivia for the rain gauge data.

Author Contributions: Frédéric Satgé, Alvaro Xavier and Marie-Paule Bonnet conceived the experiments and analyzed the data. Jérémie Garnier, Ramiro Pillco Zolá, Yawar Hussain and Franck Timouk contributed in resolving problems during the data processing and interpretation. Frédéric Satgé and Marie-Paule Bonnet wrote the paper.

Conflicts of Interest: The authors declare no conflict of interest.

References

1. Liu, Z. Comparison of Integrated Multisatellite Retrievals for GPM (IMERG) and TRMM Multisatellite Precipitation Analysis (TMPA) Monthly Precipitation Products: Initial Results. *J. Hydrometeorol.* **2016**, *17*, 777–790. [CrossRef]
2. Prakash, S.; Mitra, A.K.; AghaKouchak, A.; Liu, Z.; Norouzi, H.; Pai, D.S. A preliminary assessment of GPM-based multi-satellite precipitation estimates over a monsoon dominated region. *J. Hydrol.* **2016**. [CrossRef]
3. Sharifi, E.; Steinacker, R.; Saghafian, B. Assessment of GPM-IMERG and Other Precipitation Products against Gauge Data under Different Topographic and Climatic Conditions in Iran: Preliminary Results. *Remote Sens.* **2016**, *8*, 135. [CrossRef]
4. Chen, F.; Li, X. Evaluation of IMERG and TRMM 3B43 Monthly Precipitation Products over Mainland China. *Remote Sens.* **2016**, *8*, 472. [CrossRef]
5. Tang, B.H.; Shao, K.; Li, Z.L.; Wu, H.; Nerry, F.; Zhou, G. Estimation and validation of land surface temperatures from chinese second-generation polar-orbit FY-3A VIRR data. *Remote Sens.* **2015**, *7*, 3250–3273. [CrossRef]
6. Müller, M.F.; Thompson, S.E. Bias adjustment of satellite rainfall data through stochastic modeling: Methods development and application to Nepal. *Adv. Water Resour.* **2013**, *60*, 121–134. [CrossRef]
7. Amani, M.; Parsian, S.; MirMazloumi, S.M.; Aieneh, O. Two new soil moisture indices based on the NIR-red triangle space of Landsat-8 data. *Int. J. Appl. Earth Obs. Geoinf.* **2016**, *50*, 176–186. [CrossRef]
8. Condom, T.; Rau, P.; Espinoza, J.C. Correction of TRMM 3B43 monthly precipitation data over the mountainous areas of Peru during the period 1998–2007. *Hydrol. Process.* **2010**, *25*, 1924–1933. [CrossRef]
9. Satgé, F.; Bonnet, M.-P.; Gosset, M.; Molina, J.; Hernan Yuque Lima, W.; Pillco Zolá, R.; Timouk, F.; Garnier, J. Assessment of satellite rainfall products over the Andean plateau. *Atmos. Res.* **2016**, *167*, 1–14. [CrossRef]
10. Blacutt, L.A.; Herdies, D.L.; de Gonçalves, L.G.G.; Vila, D.A.; Andrade, M. Precipitation comparison for the CFSR, MERRA, TRMM3B42 and Combined Scheme datasets in Bolivia. *Atmos. Res.* **2015**, *163*, 117–131. [CrossRef]
11. Satgé, F.; Bonnet, M.P.; Timouk, F.; Calmant, S.; Pillco, R.; Molina, J.; Lavado-Casimiro, W.; Arsen, A.; Crétaux, J.F.; Garnier, J. Accuracy assessment of SRTM v4 and ASTER GDEM v2 over the Altiplano watershed using ICESat/GLAS data. *Int. J. Remote Sens.* **2015**, *36*, 465–488. [CrossRef]
12. Satge, F.; Denezine, M.; Pillco, R.; Timouk, F.; Pinel, S.; Molina, J.; Garnier, J.; Seyler, F.; Bonnet, M.-P. Absolute and relative height-pixel accuracy of SRTM-GL1 over the South American Andean Plateau. *ISPRS J. Photogramm. Remote Sens.* **2016**, *121*, 157–166. [CrossRef]
13. Kummerow, C.D.; Randel, D.L.; Kulie, M.; Wang, N.Y.; Ferraro, R.; Joseph Munchak, S.; Petkovic, V. The evolution of the goddard profiling algorithm to a fully parametric scheme. *J. Atmos. Ocean. Technol.* **2015**, *32*, 2265–2280. [CrossRef]
14. Ushio, T.; Sasashige, K.; Kubota, T.; Shige, S.; Okamoto, K.; Aonashi, K.; Inoue, T.; Takahashi, N.; Iguchi, T.; Kachi, M.; et al. A Kalman Filter Approach to the Global Satellite Mapping of Precipitation (GSMaP) from Combined Passive Microwave and Infrared Radiometric Data. *J. Meteorol. Soc. Jpn.* **2009**, *87*, 137–151. [CrossRef]
15. Yamamoto, M.K.; Shige, S. Implementation of an orographic/nonorographic rainfall classification scheme in the GSMaP algorithm for microwave radiometers. *Atmos. Res.* **2014**, *163*, 36–47. [CrossRef]
16. Huffman, G.J.; Bolvin, D.T. *TRMM and Other Data Precipitation Data Set Documentation*; NASA/GSFC: Greenbelt, MD, USA, 2014.
17. Taylor, K.E. Summarizing multiple aspects of model performance in a single diagram. *J. Geophys. Res.* **2001**, *106*, 7183–7192. [CrossRef]
18. Oliveira, R.; Maggioni, V.; Vila, D.; Morales, C. Characteristics and Diurnal Cycle of GPM Rainfall Estimates over the Central Amazon Region. *Remote Sens.* **2016**, *8*, 544. [CrossRef]
19. Hussain, Y.; Satge, F. Performance of CMORPH, TMPA and PERSIANN rainfall datasets over plain, mountainous and glacial regions of Pakistan. *Theor. Appl. Climatol.* **2017**, 1–14. [CrossRef]
20. Prakash, S.; Sathiyamoorthy, V.; Mahesh, C.; Gairola, R.M. An evaluation of high-resolution multisatellite rainfall products over the Indian monsoon region. *Int. J. Remote Sens.* **2014**, *35*, 3018–3035. [CrossRef]

21. Scheel, M.L.M.; Rohrer, M.; Huggel, C.; Santos Villar, D.; Silvestre, E.; Huffman, G.J. Evaluation of TRMM Multi-satellite Precipitation Analysis (TMPA) performance in the Central Andes region and its dependency on spatial and temporal resolution. *Hydrol. Earth Syst. Sci.* **2011**, *15*, 2649–2663. [CrossRef]
22. Katiraie-Boroujerdy, P.-S.; Nasrollahi, N.; Hsu, K.; Sorooshian, S. Evaluation of satellite-based precipitation estimation over Iran. *J. Arid Environ.* **2013**, *97*, 205–219. [CrossRef]
23. Ochoa, A.; Pineda, L.; Crespo, P.; Willems, P. Evaluation of TRMM 3B42 precipitation estimates and WRF retrospective precipitation simulation over the Pacific–Andean region of Ecuador and Peru. *Hydrol. Earth Syst. Sci.* **2014**, *18*, 3179–3193. [CrossRef]
24. Roebber, P.J. Visualizing Multiple Measures of Forecast Quality. *Weather Forecast.* **2009**, *24*, 601–608. [CrossRef]
25. Espinoza, J.C.; Marengo, J.A.; Ronchail, J.; Carpio, J.M.; Flores, L.N.; Guyot, J.L. The extreme 2014 flood in south-western Amazon basin: The role of tropical-subtropical South Atlantic SST gradient. *Environ. Res. Lett.* **2014**, *9*, 124007. [CrossRef]
26. Espinoza, J.C.; Chavez, S.; Ronchail, J.; Junquas, C.; Takahashi, K.; Lavado, W. Rainfall hotspots over the southern tropical Andes: Spatial distribution, rainfall intensity, and relations with large-scale atmospheric circulation. *Water Ressour. Res.* **2015**, *51*, 3459–3475. [CrossRef]
27. Satgé, F.; Espinoza, R.; Zolá, R.; Roig, H.; Timouk, F.; Molina, J.; Garnier, J.; Calmant, S.; Seyler, F.; Bonnet, M.-P. Role of Climate Variability and Human Activity on Poopó Lake Droughts between 1990 and 2015 Assessed Using Remote Sensing Data. *Remote Sens.* **2017**, *9*, 218. [CrossRef]
28. Tian, Y.; Peters-Lidard, C.D.; Eylander, J.B.; Joyce, R.J.; Huffman, G.J.; Adler, R.F.; Hsu, K.-L.; Turk, F.J.; Garcia, M.; Zeng, J. Component analysis of errors in satellite-based precipitation estimates. *J. Geophys. Res.* **2009**, *114*, D24101. [CrossRef]
29. Gebregiorgis, A.S.; Hossain, F. Understanding the Dependence of Satellite Rainfall Uncertainty on Topography and Climate for Hydrologic Model Simulation. *IEEE Trans. Geosci. Remote Sens.* **2013**, *51*, 704–718. [CrossRef]
30. Yang, Y.; Luo, Y. Evaluating the performance of remote sensing precipitation products CMORPH, PERSIANN, and TMPA, in the arid region of northwest China. *Theor. Appl. Climatol.* **2014**, *118*, 429–445. [CrossRef]